Fixed bed membrane reactor for hydrogen production from steam methane reforming: Experimental and modeling approach

Gioele Di Marcoberardino*, Francesco Sosio, Giampaolo Manzolini, Stefano Campanari

Politecnico di Milano, Dipartimento di Energia, Via Lambruschini 4, 20156 Milano, Italy

This work describes the results from experimental tests on the membrane reactor in terms of hydrogen recovery factor and fuel conversion at different operating conditions. A test bench for a fixed bed membrane reactor, placed in the Laboratory of Micro-Cogeneration (LMC) of Politecnico di Milano, is designed to operate in a wide range of operating condi-tions: the maximum temperature and pressure are respectively 923 K and 700 kPa. An hydrogen permeability value of 5.16 10^{-11} mol/(msPa$^{0.71}$) at 723 K have been determined. The best operating conditions (873 K, 500 kPa) allow to reach a methane conversion of 47.4% and an hydrogen recovery factor of 28.1%. Results are used to validate a one-dimensional finite volume model of the overall membrane reactor, solved in Matlab®.

Keywords:
Hydrogen
Membrane reactor
Fixed bed
Palladium membrane One-dimensional model Steam methane reforming

Introduction

The current topics of energy saving and reduction of CO_2 emissions must deal with the significant energy demand in residential area. Indeed electricity and heat consumptions, in industrialized countries, are responsible for a large share of consumption of primary energy. In this context, an increasing interest has been built up on innovative solutions for small scale power generation, focusing on the field of Proton Exchange Membrane fuel cell (PEMFC) based systems, potentially characterized by high net electric efficiency and very low emissions targeting the application to distributed heat and power co-generation (CHP) in the urban areas.

Fuel cells have high electric efficiencies even at small scale together with low pollution emissions. The PEM cell type also have (i) a high power density, (ii) a fast start and (iii) low operating temperatures. All these advantages lead to say that the production of electric energy, through a fuel cell system, can allow low costs and high efficiencies even on a range of net electric power output that goes from 100 to 3000–5000 W, corresponding to the energy needs of a residential user.

The main disadvantage of the PEM cells is that they require high purity hydrogen as fuel, with CO concentration below 10 ppm (at least for the LT-PEM type). Since there isn't a hydrogen distribution network nowadays, the vast majority of PEM-based CHP systems are fed with natural gas which is widely present in major cities; moreover, the use of other fuels as bio-ethanol is of growing interest for stand-alone and off-

* *Corresponding author*. Tel.: +39 02 2399 3935.
E-mail address: gioele.dimarcoberardino@polimi.it (G. Di Marcoberardino).

Published Journal Article available at: http://dx.doi.org/10.1016/j.ijhydene.2014.11.045

grid locations. So these systems require a fuel processor upstream the fuel cell.

In this context, palladium alloy membranes are a promising technology for integration into a fuel processor involving pure hydrogen generation from a liquid or gas fuel. In the field of hydrogen-selective membranes, they feature high permse-lectivity but limited permeation flux as well as the ability to operate at high temperatures and pressures [1]. The advantages of this innovative solution are both economic (conversion and separation take place in a single reactor), and thermodynamic: the hydrogen production and separation are performed mini-mizing temperature swing with energy and exergetic advan-tages [2]. These characteristics make membranes suitable for small-scale stationary generation based on PEM fuel cell sys-tem [3–5].

This work analyzes the performances of a fixed bed membrane reactor in terms of hydrogen production rate and methane conversion at different operating conditions, which were compared with some experimental and prediction results appearing in the literature. Experimental data are used to validate a mathematical model in terms of kinetics reactions efficiency. Results were compared with some prediction re-sults appearing in the literature.

Membrane reactor model

The flexibility of the finite volumes 1D model in Matlab® gives the opportunity to simulate a wide variety of membrane reactor configurations differing in geometry, flow patterns and re-actants composition. The model considers the system at steady state conditions and the velocity profiles are in first approxi-mation fully developed in the entry region. Therefore, the pro-files of the variables are determined along the z-coordinate alone, corresponding to the length of the reactor, as shown in Fig. 1. The differential equations are traced to polynomial ex-pressions where the unknowns are functions of the coordinate z. Starting from the input data of the system (geometric pa-rameters, inlet stream and his composition and the reactor operating conditions), the numerical model calculates the main variables trend: the composition (or the molar flow rates of the chemical species) and the temperature of the mixtures that pass through the reactor. The process is governed by the ma-terial balance and energy balance: these have been written for both the reaction zone and the permeating zone.

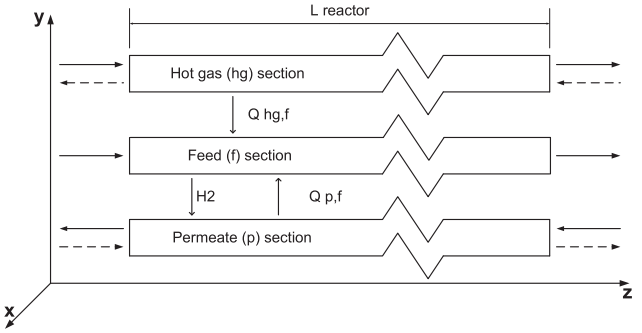

Fig. 1 – Scheme of 1D Membrane Reactor model.

Regarding the mass balance on the feed section implemented in the 1D model, the reaction equations, kinetic and adsorption parameters have been extracted fromXu & Froment [6]: all parameters are summarized in Table 1. The terms η1and η2 are defined as the kinetic efficiency for the first two reactions: experimental results are used to validate the numerical model through the evaluation of these costants (chapter 4.3).

The expression to calculate the hydrogen permeation flux through the membrane J_{H_2} [mol/m^{2}s] is shown in Eq. (1). Hydrogen flux is a function of the hydrogen partial pressure difference between feed and permeate sides and of the reaction temperature.

$$J_{H_2} = \frac{P_0 \cdot e^{-Ea/RT}}{t} \cdot \left(p_F^n - p_P^n\right) \tag{1}$$

The term inside the bracket is the driving force [kPa^n]. Eq. (2) shows the mass balance equations in the feed section for all species (i) and reaction product/reagents (j), expressed in mol/m·s, where, the term J_i differs from zero only for the hydrogen, by using a membrane infinitely selective to hydrogen (assumed in this study).

$$\frac{dN_i}{dz} = \rho_{cat}\frac{V}{L} \cdot \sum_{j=1}^{3} \upsilon_{ij} r_j - J_i \cdot \frac{S_{mem}}{L_{mem}} \qquad \text{where} \quad i = 1, \ldots, n_{species} \tag{2}$$

As explained above, differential equations are traced to a polynomial expression along the coordinate z: Eq. (3) defines the mass balance, expressed in mol/s, where the reactor is divided in several cells with a definite volume length L_k.

$$N_{i,k}^{OUT} = N_{i,k}^{IN} + \frac{V}{L} L_k \cdot \rho_{cat} \cdot \left(\sum_{j=1}^{3} \upsilon_{ij} r_j\right)_k - J_{i,k} \cdot \pi D_{mem} \cdot L_k$$
$$\text{where} \quad k = 1, \ldots, n_{cells} \& n_{cells} = \frac{L_k}{L} \tag{3}$$

The same mass balance is also used for the permeate and hot gas sections: in the first, r_j is equal to 0 and the hydrogen permeated flux has the opposite sign, while, in the hot gas stream both reaction term and permeation term are not take into account.

For the energy balance, there is a set of equations for the three sections of the reactor: the hot gas, the feed and the permeate. The energy balance, expressed in Watt, in the feed section is presented in Eq. (4).

$$H_{out,f}\left(T_{f,k+1}\right) = H_{in,f}\left(T_{f,k}\right) + Q_{hg,f}\left(T_{hg,k}\right) + Q_{p,f}\left(T_{p,k}\right) + H_{H_2,p,k} \tag{4}$$

where the terms $Q_{hg,f}$ and $Q_{p,f}$ stand for the conductive heat transfer between the feed flow and the hot gas and the feed and permeate flows respectively; the term $H_{H_2,p}$ refers to the heat transport of the hydrogen permeate flux as shown in Eq. (5).

$$H_{H_2,p,k} = J_{H_2,k} \cdot S_{mem,k} \cdot MM_{H_2} \cdot \int_{298K}^{T_{f,k}} C_{p,H_2}(T)\,dT \tag{5}$$

Experimental setup and tests

Membrane reactor test bench

The membrane reactor test bench is shown in Fig. 2. The membrane reactors can be fed with three different gases, CH_4,

Table 1 – Reaction equations, kinetic and adsorption parameters.

$CH_4 + H_2O = CO + 3H_2$	ΔH (298 K) = 206 kJ/mol R.1
$CO + H_2O = CO_2 + H_2$	ΔH (298 K) = −41 kJ/molR.2
$CH_4 + 2H_2O = CO_2 + 4H_2$	ΔH (298 K) = 165 kJ/mol R.3
$r_1 = \eta_1 \cdot \frac{\frac{k_1}{p_{H_2}^{2.5}} \cdot \left(p_{CH_4} \cdot p_{H_2O} - \frac{p_{H_2}^3 \times p_{CO}}{k_{eq1}} \right)}{DEN^2}$	$k_1 = 371.1 \cdot 10^{15} \cdot e^{\left(\frac{2.401 \cdot 10^5}{RT}\right)}$ $k_{eq1} = 119.8 \cdot 10^{21} \cdot e^{\left(\frac{-26830K}{T}\right)}$
$r_2 = \eta_2 \cdot \frac{\frac{k_2}{p_{H_2}} \cdot \left(p_{CO} \cdot p_{H_2O} - \frac{p_{H_2} \cdot p_{CO_2}}{k_{eq2}} \right)}{DEN^2}$	$k_2 = 5.431 \cdot e^{\left(\frac{6.713 \cdot 10^4}{RT}\right)}$ $k_{eq2} = 1.767 \cdot 10^{-2} \cdot e^{\left(\frac{4400K}{T}\right)}$
$r_3 = \frac{\frac{k_3}{p_{H_2}^{3.5}} \cdot \left(p_{CH_4} \cdot p_{H_2O}^2 - \frac{p_{H_2}^4 \cdot p_{CO_2}}{k_{eq3}} \right)}{DEN^2}$	$K_3 = 89.6 \cdot 10^{15} \cdot e^{\left(\frac{24.39 \times 10^4}{RT}\right)}$ $k_{eq3} = k_{eq1} \cdot k_{eq2}$
where $DEN = 1 + k_{H_2} \cdot p_{H_2} + k_{CH_4} \cdot p_{CH_4} + k_{CO} \cdot p_{CO} + k_{H_2O} \cdot \frac{p_{H_2O}}{p_{H_2}}$	
$k_{H_2} = 6.12 \cdot 10^{-14} \cdot e^{\left(\frac{82.9 \cdot 10^3 J/mol}{RT}\right)}$	$k_{CO} = 8.23 \cdot 10^{-10} \cdot e^{\left(\frac{70.65 \cdot 10^3 J/mol}{RT}\right)}$
$k_{CH_4} = 6.65 \cdot 10^{-9} \cdot e^{\left(\frac{38.28 \cdot 10^3 J/mol}{RT}\right)}$	$k_{H_2O} = 1.77 \cdot 10^5 \cdot e^{\left(\frac{-88.68 \cdot 10^3 J/mol}{RT}\right)}$

N_2 and H_2, controlled by mass flow controllers and steam supplied by means of a digital-dosing diaphragm pump. Steam and gases are mixed into an electrically traced pipeline before entering the reactor from the top. The reactor pressure is controlled by using pressure transmitters and a modulating backpressure valve located in the retentate outlet pipeline. The maximum working pressure of the reactor is 10 bar (pressure limit changes with the working temperature for safety reasons), while the permeate side is at ambient pressure. The maximum operating temperature (to maintain membrane stability) is 923 K. From the reactor outlet, hot gases, both permeate and retentate line, are cooled down (and condensate separated for the retentate stream). So the gas analysis section consists of mass flow meters that measure the exit gas flows and of a micro gas chromatograph to analyze the molar composition of the retentate.

The reactor has 10 commercial dead-end membrane tubes of 3.18 mm outside diameter and 200 mm length and it is filled with 130 g of a CPO catalyst $Ni-Al_2O_3$ (supplied by REB [7]). The membrane consists of a porous metal support reinforced with Inconel, having two $Pd_{0.77}-Ag_{0.23}$ layers: the one on the outer surface is 3.0 μm thick, while the layer on the inner surface is of 1.5 μm. The 10 tubes are welded by their open ends to a plate manifold. A scheme of the fixed bed membrane reactor is shown in Fig. 3.

The reactor has an internal diameter of 21.2 mm and a length of 510 mm. It is externally heated by 850 W electric furnace. The temperature inside the bed is measured in three different positions (at the top, middle and bottom of the membrane tube), and it is controlled modulating the furnaces power output. Permeate from each tube is collected at the bottom of the reactor.

Measurements are recorded at steady state condition, which are verified against the stability of (i) the retentate composition, (ii) the gas temperature inside the chamber, (iii) the outlet flow stability, and (iv) the reactor operating pressure; operating pressure must remain within 1 kPa range from the setpoint. The duration of the acquisition is related to the entire system inertia and to the data collected by the gas chromatograph. The latter requires more time because for the acquisition of 20 measurements one to one and half hour is necessary. The recorded data are filtered statistically and used to close the carbon mass balance. Every test was repeated at least one time to verify the reproducibility of the results.

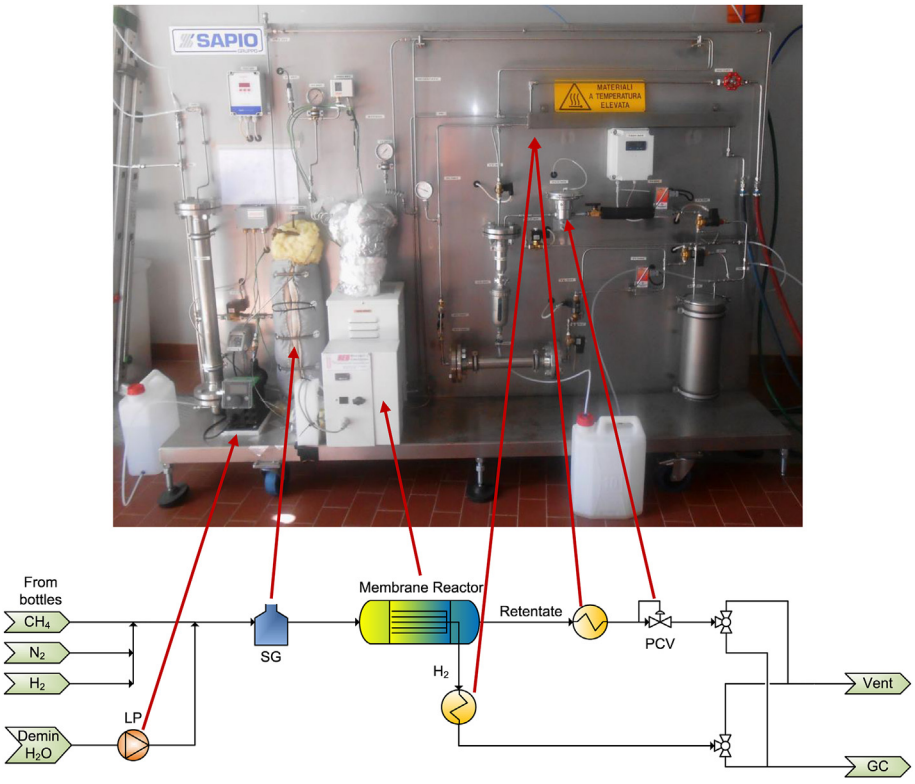

Fig. 2 – Membrane reactor test bench and its process flow diagram (PFD).

Hydrogen permeation test

Performances of a membrane reactor strictly depend on the membrane characteristics as the permeability and the selectivity. The membrane permeability coefficients (*Ea*, P_0 and *n* in Eq. (1)) are calculated starting from the flow rate measurements of the permeated hydrogen. The transmembrane flux typically depends on temperature, showing higher values at higher temperatures. The exponent *n* of the partial pressures of hydrogen depend on the rate limiting step of permeation pro-cess, and is experimentally determined to be in the 0.5–1.0 range: usually *n* is equal to 0.5 for dense membrane with a thickness between 7 and 10 μm, where the diffusion of hydrogen atoms through the palladium is rate-limiting; while, for thinner membranes (3–5 μm), the value of *n* approaches 1 [8].

Pure hydrogen feeding at different hydrogen partial pressures and temperatures were considered for the calculation of *Ea* and P_0. Different reactor operating conditions were investigated by varying the hydrogen partial pressure and gas temperatures. The behavior of the membrane was investigated in the range of operating conditions with temperature from 723 to 798 K and absolute pressures from 300 to 550 kPa but at constant driving force.

Reaction test

Reaction tests were conducted to analyze the membrane reactor behavior and, especially, his performance in terms of fuel conversion (Eq. (6)) and Hydrogen Recovery Factor (HRF) (Eq. (7)).

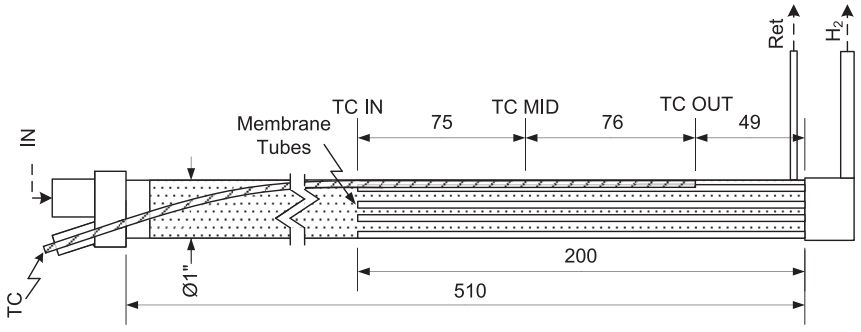

Fig. 3 – Membrane reactor setup.

Table 2 – Operating conditions reaction tests.

Flow CH_4 inlet [mol/s]		T reactor [K]			
		773	823	848	873
P reactor [kPa]	400	$3.72\cdot10^{-4}$	$3.72\cdot10^{-4}$	$3.72\cdot10^{-4}$	$3.72\cdot10^{-4}$
		$7.44\cdot10^{-4}$	$7.44\cdot10^{-4}$	$7.44\cdot10^{-4}$	$7.44\cdot10^{-4}$
	500	$3.72\cdot10^{-4}$	$3.72\cdot10^{-4}$	$3.72\cdot10^{-4}$	$3.72\cdot10^{-4}$
		$7.44\cdot10^{-4}$	$7.44\cdot10^{-4}$	$7.44\cdot10^{-4}$	$7.44\cdot10^{-4}$
	600	$3.72\cdot10^{-4}$	$3.72\cdot10^{-4}$	$3.72\cdot10^{-4}$	$3.72\cdot10^{-4}$
		$7.44\cdot10^{-4}$	$7.44\cdot10^{-4}$	$7.44\cdot10^{-4}$	$7.44\cdot10^{-4}$
	700	$3.72\cdot10^{-4}$	$3.72\cdot10^{-4}$	$3.72\cdot10^{-4}$	$3.72\cdot10^{-4}$
		$7.44\cdot10^{-4}$	$7.44\cdot10^{-4}$	$7.44\cdot10^{-4}$	$7.44\cdot10^{-4}$

$$X_{CH_4} = \frac{N_{CH_4,f,in} - N_{CH_4,f,out}}{N_{CH_4,f,in}} \quad (6)$$

$$HRF = \frac{N_{H_2,p}}{4\cdot N_{CH_4,f,in} + N_{H_2,f,in}} \quad (7)$$

A preliminary investigation allowed determining the range of reactor operating conditions. Table 2 shows the operating conditions for the reaction tests. In all tests, it was chosen a value of steam to carbon (S/C) of 3 in order to avoid carbon deposition on the catalyst and membrane surfaces [9].

Two different experimental campaigns were carried out. The first focused on the catalyst efficiency and reaction kinetics: the steam reforming (SR) and water gas shift (WGS) reactions were evaluated setting the driving force is imposed to zero (DF = 0) by closing an in-line 2-way valve on the permeate side. In the second study, the permeate side was open to the ambient in order to evaluate the enhanced reaction performance due to the hydrogen separation by the Pd–Ag membrane. Moreover reaction tests differ in the methane flow fed into the reactor: so it can be determined the effect of the weighted hourly space time (WHST).

Results and discussion

Membrane characteristics

Fig. 4(a) shows the measured permeate flow at different driving forces at 723 K and assuming different exponents *n*. The lower least-squares error occurs for a value of *n* equal to 0.71.

Therefore, the activation energy and the pre-exponential factor could be determined with hydrogen permeation tests at different working temperature and keeping the same driving force: they resulted to be 6.99 kJ/mol and $1.65\cdot10^{-10}$ mol/(msPa$^{0.71}$), respectively. Fig. 4(b) shows the hydrogen flux resulting from Eq. (1) for all tests versus the measured flux: this reveals that the determined parameters fit also at different operating conditions. The comparison with other experimental results of similar Pd–Ag membranes confirms that the membrane behavior in terms of permeance is consistent with avail-able literature data [10,11]: the activation energy is in the range of 5–16 kJ/mol, while the values for P_0 order go from $1\cdot10^{-7}$ to $2\cdot10^{-11}$ (this parameter also depends on the exponent n).

Membrane reactor behavior

Although the values of methane conversion are not very high, results of reaction tests (i.e. DF = 0), in Fig. 5(a and b), show the positive influence of higher WHST and temperature on the methane conversion: the higher space time favors the reactants diffusion inside the catalyst surface reducing the unconverted feed flow that crosses through the fixed bed. On the other hand the increase of operating pressure has an opposite effect. Anyway the low X_{CH_4} values measured in this study (from 10% to 25%) are due to the temperature inlet of reactants that is about 423–433 K: the first section of the reactor works only as preheater, as shown in Fig. 6.

The objective of the second study was to assess the benefits of product subtraction to SR and WGS reactions. The continuous removal of the hydrogen from the retentate, due to the presence of the Pd–Ag membrane, causes an imbalance of the reactions towards the products ensuring better yields.

Main attention is given to the effect of the operating pressure on the reactor: although this parameter adversely affects the reforming reactions, it should enhance the flux of the membrane. These tests are useful for identifying the most critical parameter on the fuel conversion. For this investigation, the CH_4 feed flow is set to $3.72\cdot10^{-4}$ mol/s, that corresponds to a WHST of 349.6 $kg_{cat}s/mol_{CH_4}$.

Fig. 7(a) proves the benefits of the membrane integration in reactors; in particular, the methane conversion rises from 23.3% to 47.4% with a significant increase respect to the results shown in Fig. 5(b). Also for the reaction tests with permeation,

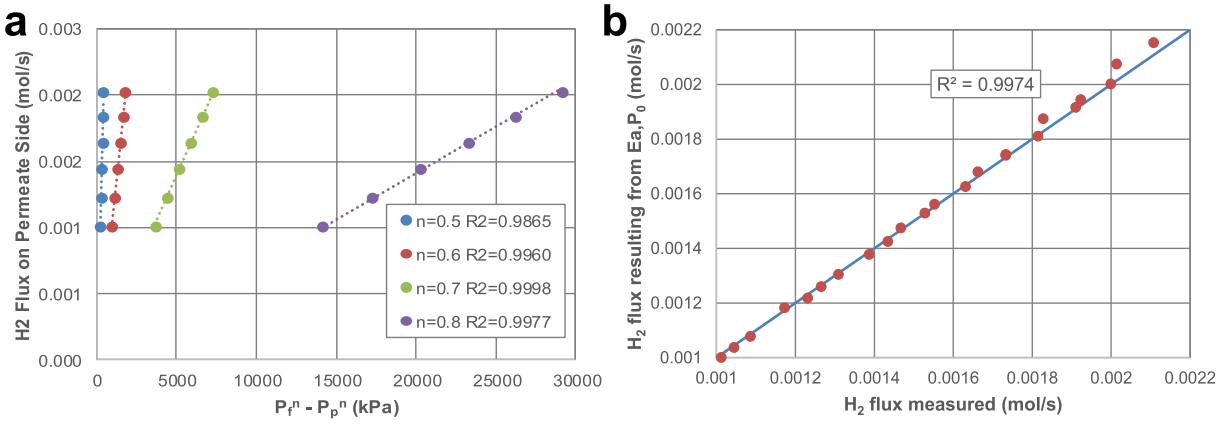

Fig. 4 – (a) Effect of driving force on H_2 flux on the permeate side assuming different exponents *n* (b) H_2 flux resulting from Eq. (1) to H_2 flux measured in permeation tests.

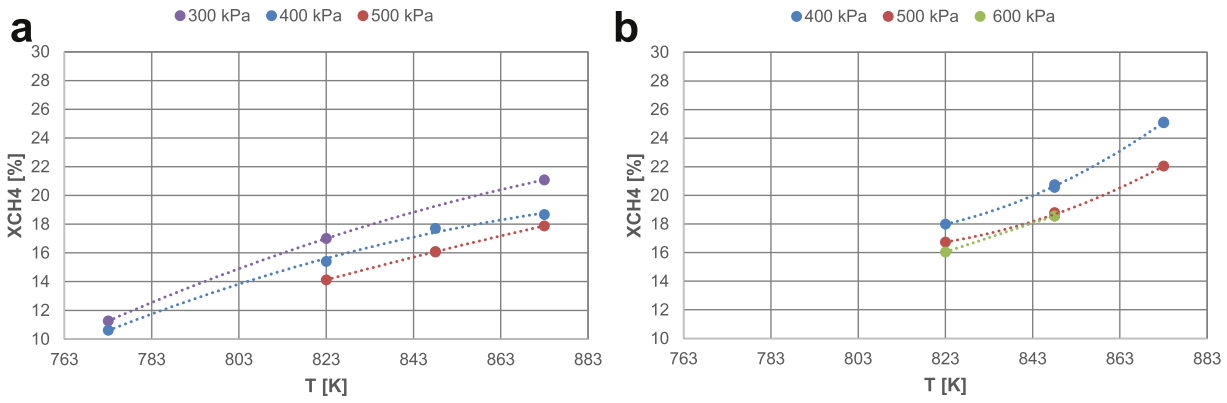

Fig. 5 – (a) Methane conversion for reaction tests with DF = 0, WHST = 174.8 $kg_{cat}s/mol_{CH_4}$ (b) Methane conversion for reaction tests with DF = 0, WHST = 349.6 $kg_{cat}s/mol_{CH_4}$.

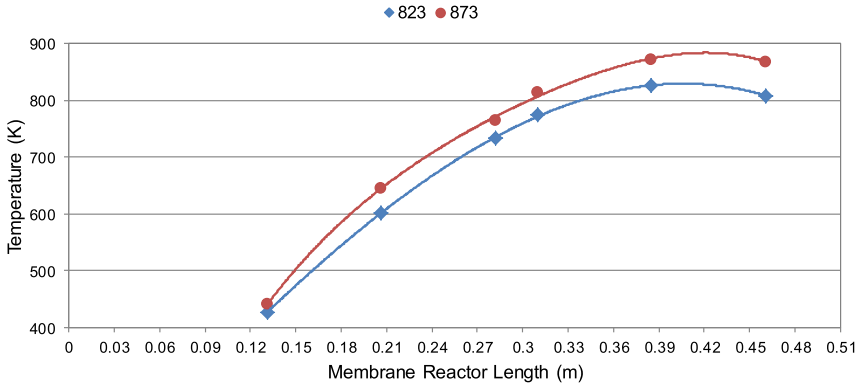

Fig. 6 – Temperature profile inside the reactor for reaction tests with DF = 0.

the increase of operating temperature has a positive influence on both kinetics of reactions and permeability of the membrane.

As observed in Fig. 8, another interesting aspect observed during the experimental investigations regards the effect of temperature on the flow of retentate and permeate: at constant pressure, the increase of temperature causes the increase of permeate flow while maintaining constant the flow rate of the retentate. This effect highlights the benefits that the increase in temperature results on the permeability of the membrane.

Furthermore Fig. 7 shows the increase of the methane conversion with reactor pressure in the second campaign. This positive trend highlights that the improved performance depends on the driving force and this effect prevails on the control of the reactor operating temperature.

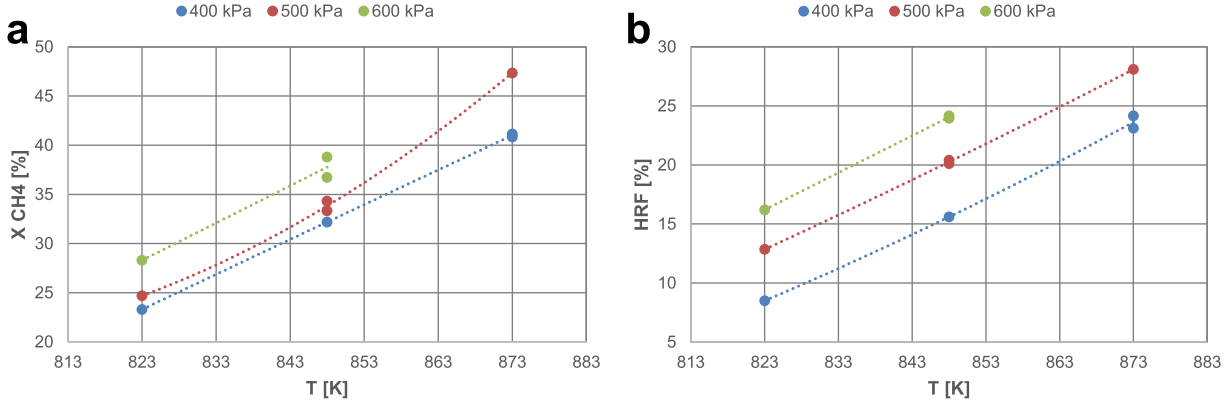

Fig. 7 – Methane conversion (a) and Hydrogen Recovery Factor (b) for reaction tests with permeation (WHST = 349.6 $kg_{cat}s/mol_{CH_4}$).

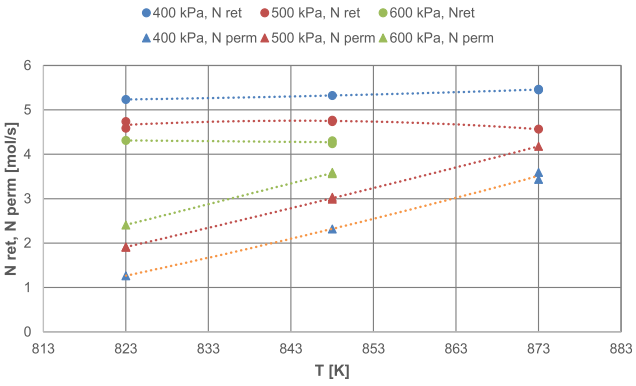

Fig. 8 – Retentate and permeate flow [mol/s] for the reaction tests with permeation.

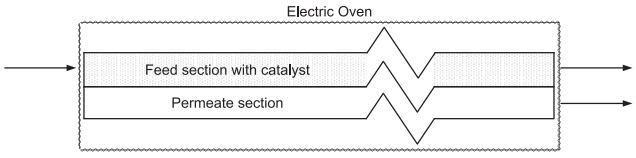

Fig. 9 – Membrane Reactor test bench in 1D model.

Table 3 – Kinetic efficiency value from 1D MR model calibration.

Kinetic efficiency for tests with DF = 0		Kinetic efficiency for tests with permeation	
$\eta 1$	0.0012	$\eta 1$	1
$\eta 2$	0.3	$\eta 2$	1

Membrane reactor model calibration

Experimental data are used to validate the 1D mathematical model in terms of kinetics reactions efficiency. The Matlab simulation program differs from the analyzed experimental device, shown in Fig. 9, by the following aspects: the current sweep gas, which in the model is used to evacuate the hydrogen permeate, is not provided for the membrane reactor studied in the laboratory; also the heat required to sustain the endothermic reactions is provided by an electric furnace and not by a flow of hot gases. Due to the complexity of the system and to the absence of significant data on the heater, the model solved the energy balance on the feed section by fixing the temperature profile along the feed side according to the measured measurements during the testing with the three internal thermocouples. Once defined geometric parameters and operating conditions, it could be calculated the kinetic efficiency ($\eta 1$ and $\eta 2$) for the reaction R.1 and R.2. Xu & Froment proposed very low values for the case of industrial reactors (reactor length of 12 m and a diameter of the pellet catalyst 0.0173 m) where it was determined values ranging from 0 to 0.03 as regards $\eta 1$; on the contrary, $\eta 2$ could have higher values [12]. The rate determining step is the reactants diffusion within the catalyst pores in the fixed bed. In this study, not only the catalyst size in the range of $8.41 \cdot 10^{-4}$–$1.49 \cdot 10^{-4}$ m, but also the preheater section have a big influence on the kinetic efficiency of the steam reforming and water gas shift reactions.

Two different couples of efficiency values are founded, one for the reaction tests with DF = 0 and one for the tests with hydrogen permeation (Table 3). In both cases, these values are in good agreement with experimental data in terms of methane conversion and HRF, as shown in Table 4. The integration of the membrane in the reactor model has a great influence on the reaction rate, due to the product subtraction.

Fig. 10 shows the simulation results with an hot gas flow and a feed inlet temperature of 673 K: it could be outlined interesting that the possibility to supply the reaction heat and the pre-heating feed section with the hot gases produced by the combustion of the retentate, instead of an electric oven, allows to improve the membrane reactor performances. Simulations were performed to evaluate the effect of the direction of hot gas flow (co-flow or counter-flow) on conversion efficiency. Simulations were performed assuming the same inlet temperature (1473 K) and the kinetic efficiency value founded in the model calibration. The counter-flow case reaches the best methane conversion: at the reactor bottom, the higher hot gas temperature increase the equilibrium conversion of the reactions. However, this phenomenon hasn't a beneficial influence on permeation: the co-flow case allows to enhance an higher HRF due to the higher overall temperature on the membrane zone.

Table 4 – Comparison between experimental and simulated values.

T [K]	P [kPa]	Test type	Parameter	Experimental value	Simulated value	Relative error [%]
823	500	DF = 0	X CH_4 [%]	17.99	15.41	−14.3
			N $H_{2,f}$ [mol/s]	$2.04 \cdot 10^{-4}$	$2.27 \cdot 10^{-4}$	11.3
848	500	DF = 0	X CH_4 [%]	20.75	19.02	−8.3
			N $H_{2,f}$ [mol/s]	$2.64 \cdot 10^{-4}$	$2.79 \cdot 10^{-4}$	5.81
873	500	DF = 0	X CH_4 [%]	25.08	24.90	−0.7
			N $H_{2,f}$ [mol/s]	$3.39 \cdot 10^{-4}$	$3.61 \cdot 10^{-4}$	6.5
848	500	Perm.	X CH_4 [%]	32.19	33.04	2.6
			HRF [%]	15.60	13.87	−11.1
873	500	Perm.	X CH_4 [%]	41.14	46.4	12.8
			HRF [%]	24.15	21.97	−9.0

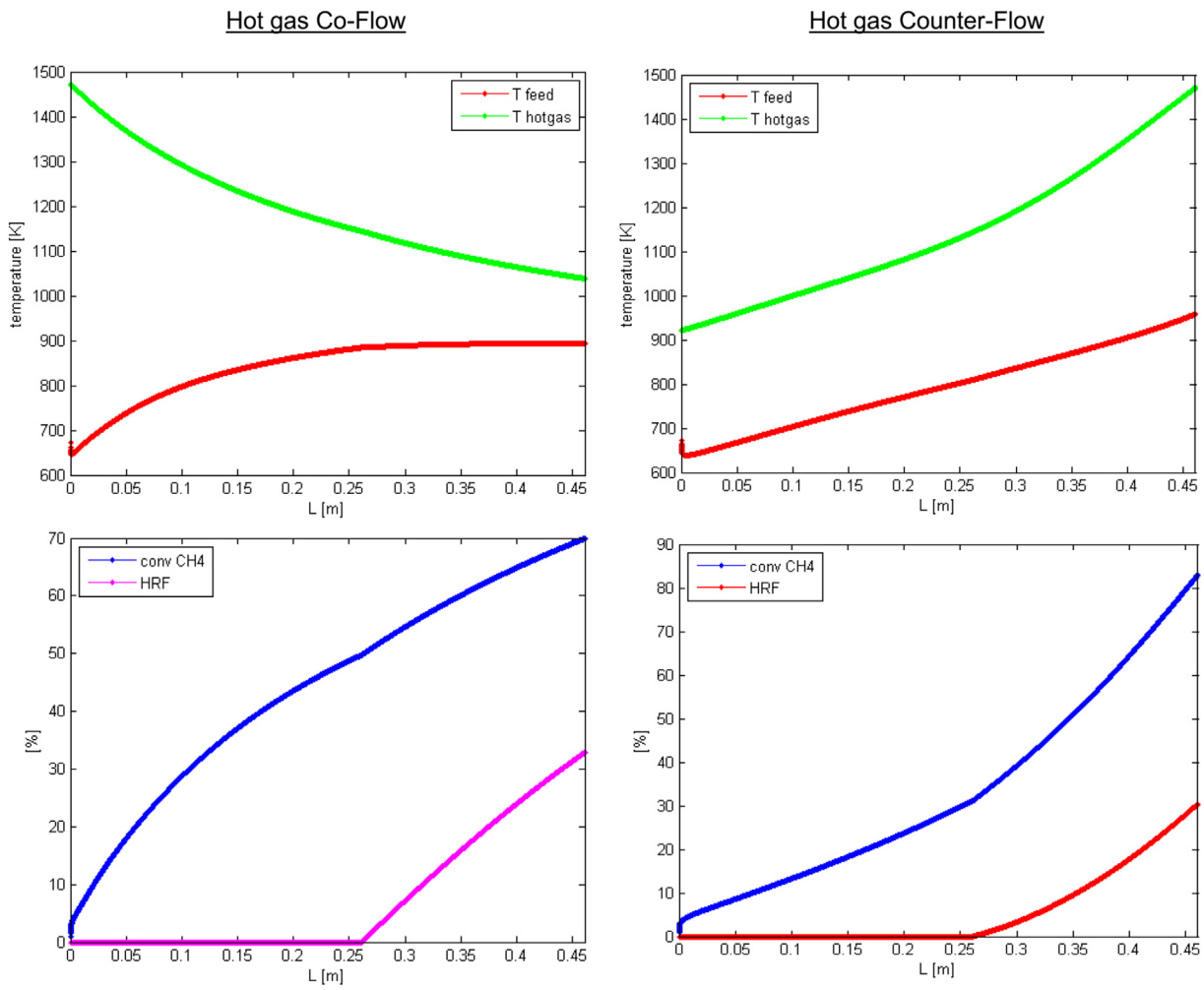

Fig. 10 – Membrane reactor performance with hot gas (co-flow and counter-flow).

Conclusions

The performance of a membrane reactor was investigated in terms of methane conversion and hydrogen recovery factor. An hydrogen permeability value of $5.16 \cdot 10^{-11}$ mol/(msPa$^{0.71}$) at 723 K have been founded for the thinner Pd–Ag membrane. The effects of operating parameters of temperature, pressure and weight hourly space time on the methane conversion and the hydrogen production rate were studied in detail. The operating temperature and the WHST had a positive effect on the membrane reactor performance. The synergetic effect of the space velocity and the operating temperature together with the operating pressure was also studied in detail. The operating pressure has a complicated effect on the methane conversion. Its effect depends on the reaction test: for the investigation with DF = 0, increasing of pressure reduce the conversion; on the other hand, the enhanced hydrogen partial pressure difference improves the conversion in the second campaign. The best operating condition (873 K, 500 kPa) allows to reach a methane conversion of 47.4% and an hydrogen recovery factor of 28.1%. The performance values measured in this study are due to the temperature inlet of reactants that is about 423–433 K: this implies that the first reaction section works only as prehaeater. Next campaing will be conducted after a new design of the preheating section.

Membrane reactor model calibration shows a good agreement with experimental data in terms of methane conversion and hydrogen recovery factor. Finally, it is shown that the possibility of working with hot gases, produced by the combustion of the retentate, and a higher feed inlet temperature allow to improve the membrane reactor performances.

Acknowledgment

This work was financially supported by national project MICROGEN 30 (Industria 2015).

Nomenclature

ΔL	length of the finite volumes, m
A	area, m^2
c_p	specific heat, J/kg K
Ea	activation energy for the permeation, J/mol
h	heat transfer coefficient, W/m^2 °C
$H_{H_2,p}$	power associate to the permeate flux,W

$H_{out,f}$	outlet power of the feed, W
HRF	hydrogen recovery factor
J_{H_2}	hydrogen permeation flux, mol/m^{2}s
J_i	i-species flux, mol/s
k_{CH_4}	Adsorption equilibrium constant of methane, Pa^{-1}
k_{CO}	adsorption equilibrium constant of carbon monoxide, Pa^{-1}
k_{H_2}	adsorption equilibrium constant of hydrogen, Pa^{-1}
k_{H_2O}	adsorption equilibrium constant of water, dimensionless
K_i	kinetic coefficient $i = 1,2,3$
$K_{eq,i}$	equilibrium constant $i = 1,2,3$
L	reactor length, m
MM	molar mass, g/mol
n	pressure exponent, dimensionless
$n_{species}$	number of species involved in the membrane reactor
n_{cells}	number of reactor finite volumes, dimensionless
p	pressure, kPa
P_0	pre-exponential permeability coefficient, mol/m^{2}s·kPa^n
p_F	hydrogen partial pressure in reaction zone, kPa
p_P	hydrogen partial pressure in permeate zone, kPa
$Q_{hg,f}$	heat exchange between hot gas and feed, W
$Q_{p,f}$	heat exchange between permeate and feed, W
R	gas universal constant, J/mol K
r_J	kinetic rate of Jth reaction, molm/kg
S_{mem}	permeation surface area, m^2
t	membrane thickness, m
T	temperature, K
V	volume, m^3
WHST	weight hourly space time, $kg_{cat}s/mol_{CH_4}$
X_{CH_4}	methane conversion, dimensionless
z	axial coordinate

Greek letters

ρ	density, kg/m^3
ν_{ij}	stoichiometric coefficient of *i*-species and *j*-reaction, dimensionless

Subscripts

F	reaction zone
f	surrounding fluid
hg	hot gas
In	inlet
mem	membrane
out	outlet
P	permeate zone

REFERENCES

[1] Paglieri SN, Way JD. Innovation in palladium membrane research. Sep Purf Rev 2002;31:1–169.

[2] Xie D, Wang Z, Jin L, Zhang Y. Energy and exergy analysis of a fuel cell based micro combined heat and power cogeneration system. Energy Build 2012;50:266–72.

[3] Campanari S, Macchi E, Manzolini G. Innovative membrane reformer for hydrogen production applied to PEM micro-cogeneration: simulation model and thermodynamic analysis. Int J Hydrogen Energy 2008;33:1361–73.

[4] Campanari S, Macchi E, Manzolini G. Membrane reformer PEM cogeneration systems for residential applications – part B: techno-economic analysis and system layout. Asia Pacific J Chem Eng 2009;4:311–21.

[5] Dorer V, Weber R, Weber A. Performance assessment of fuel cell micro-cogeneration systems for residential buildings. Energy Build 2005;37:1132–46.

[6] Xu J, Froment GF. Methane steam reforming, methanation and water-gas shift: I. Intrinsic Kinetics. AIChE J 1989;35:88–96.

[7] http://www.rebresearch.com; REB Research and Consulting.

[8] Dittmeyer R, Höllein V, Daub K. Membrane reactors for hydrogenation and dehydrogenation processes based on supported palladium. J Mol Catal A Chem 2001;173:135–84.

[9] Rostrup-Nielsen J. Catalytic steam reforming. In: Anderson, Boudart, editors. Catalysis science and technology. Springer; 1984. p. 1–117.

[10] Tong J, Matsumura Y, Suda H, Haraya K. Experimental study of steam reforming of methane in a thin (6 μm) Pd-based membrane reactor. Ind Eng Chem Res 2005;44:1454–65.

[11] Chen Y, Wang Y, Xu H, Xiong G. Efficient production of hydrogen from natural gas steam reforming in palladium membrane reactor. Appl Catal B Environ 2008;81:283–94.

[12] Xu J, Froment GF. Methane steam reforming: II. Diffusional limitations and reactor simulation. AIChE J 1989;35:97–103.